MEASUREMENT OF THE EXCITATION FUNCTIONS FOR THE FORMATION OF SEVERAL FISSION PRODUCTS BY α-PARTICLE INDUCED FISSION OF GOLD

By P. Jahn, H. J. Probst, C. Alderliesten* and C. Mayer-Böricke

Institut für Kernphysik, Kernforschungsanlage Jülich, D-5170 Jülich, W. Germany

(Received March 28, 1983)

The excitation functions for the production of ^{84}Rb, ^{86}Rb, ^{95}Zr (cumulative), ^{95}Nb, ^{103}Ru (cumulative) and ^{110m}Ag by ^{197}Au (α, f) have been measured in the energy range 65 MeV $\leqq E_\alpha \leqq$ 155 MeV using the stacked-foil technique. The data for $A = 95$ represent almost the total yield for this mass chain; adopting the charge-distribution width parameter value $c = 0.95$ from the literature the energy dependence of the most probable nuclear charge was derived.

PACS numbers: 25.85.Ge

1. Introduction

Excitation functions of (particle, *xnyp*) reactions on gold have been studied in our laboratory using the simple but efficient stacked-foil method with γ-ray spectrometry of the residual nuclei. Data for α-particle induced reactions can be found in Ref. [1]. Experimental total cross sections for fission of gold by α-particles with energies up to 120 MeV were reported by Moretto [2]. Above 100 MeV, they are only one order of magnitude smaller than those for (α, *xnyp*) reactions.

The stacked-foil technique without more sophisticated radiochemical or mass-spectrometric methods can therefore in principle be suited for the measurement of certain fission products. Its main advantage consists in covering an appreciable energy range with one single irradiation. The identification of specific nuclei by their γ-ray spectra can be useful in the study of the mass and charge distributions resulting from the fission process. On the other hand, however, this method is restricted in our case to fission products with half-lives of more than a few days because of the high background from the shorter-lived evaporation products. By that, the number of cases where more than one member of an isobaric chain can be measured is strongly reduced and consequently the information obtained concerning the charge distribution is only limited.

* Present address: Fysisch Laboratorium, Rijksuniversiteit, Utrecht, The Netherlands.

In this work the excitation functions for the formation of several fission products from $^{197}Au+\alpha$ in the mass range $84 \leqslant A \leqslant 110$ (nearly symmetric fission region) and with half-lives of the order of weeks and months were measured over the 65–155 MeV incident α-energy range. For $A = 95$, one cumulative and one independent yield curve could be determined which permits — to a certain extent — an analysis with regard to the charge distribution as a function of the α-particle energy.

2. Experimental

The stack which was irradiated in this experiment consisted mainly of Au and Cu foils, alternately mounted in an aluminium holder. The thicknesses of the foils were determined by weighing and were found to be 20 μm and 87 μm for the Au and Cu foils, respectively. In addition, two Al monitor foils, each 98 μm thick, were inserted at positions corresponding to $E_\alpha = 100$ and 92 MeV. Finally, a 54 μm Al foil was put in front of the stack. The diameter of all foils was 16 mm.

The stack was irradiated for ten hours with a 156 MeV α-particle beam of $i_\alpha = 0.8$ μA. The external unanalysed beam (relative energy width $\Delta E/E = 3 \cdot 10^{-3}$) of the isochronous cyclotron JULIC was used. A copper collimator with a borehole of 4 mm diameter, just in front of the stack, served as an indicator for the beam focussing. The beam transport magnets were adjusted to minimize the fraction of the beam hitting the collimator to a negligible amount. Just before the irradiation of the stack a single 54 μm thick Al foil was irradiated under the same conditions, but for a shorter period; the total beam charge was measured in this run using a Faraday cup and a beam-current integrator. The activities of this foil and of the 54 μm Al foil at the high-energy end of the stack were used to determine the mean beam current of the stack irradiation. An independent determination of this quantity was obtained with the help of the Al monitor foils mentioned above.

The γ-ray activities of the foils were measured with a conventional Ge(Li)-spectrometer (80 cm^3 active volume) in well-defined and reproducible geometries. Calibration spectra of ^{152}Eu and IAEA standard sources were taken in the same geometries. The energy resolution was typically 2.6 keV (FWHM) at $E_\gamma = 1.33$ MeV. The spectra with a length of 2k channels were stored on magnetic tape for further analysis. All Au foils were measured three, fifteen and thirty days after irradiation. At the time of the first series the spectrometry of the Al foils was done, whereas some of the Cu degraders were measured at the time of the third series in order to check the escape of fission products from the Au foils.

3. Data reduction and results

The areas and energies of the peaks in the γ-ray spectra were determined with a PDP-15 computer using a modified version of the program described in Ref. [3]: Multiplets with up to five components could be treated; the background was linearly interpolated and subtracted; Gaussians with exponential low-energy tails were fitted to the experimental data. The energy calibration as well as the line-shape parameters and the relative efficiency

as functions of γ-ray energy were obtained from the ^{152}Eu spectra. Relative intensities of the ^{152}Eu-decay γ-lines were taken from the literature [4]. The absolute scale was determined using the spectra of the standard sources.

The spectroscopic data of the fission products relevant for the yield curves measured in this work are listed in Table I. Points of special care were the identity and the purity

TABLE I

Spectroscopic data of fission products[a]

Fission product	Half-life (days)	E_γ (keV)	Abundance (photons per 100 decays)
^{84}Rb	33.0	881.5	73.4
^{86}Rb	18.66	1076.63[b]	8.8
^{95}Zr	65.5	724.18	43.0
		756.72	54.6
^{95}Nb	35.1	765.79	99
^{103}Ru	39.6	497.08	90
^{110m}Ag	253	657.74	93.8

[a]From Ref. [5].

[b]The value given for ^{86}Rb decay (E_γ = 1078.8 keV [5]) fits worse with our data, so we prefer the value given for ^{86}Y decay [5].

of the γ-peaks from which cross sections were to be calculated. Data from different measuring series and cross-section and half-life considerations as well as the γ-ray tables of Bowman and MacMurdo [5] were used to rule out all alternatives or significant contaminations, especially those originating from ^{197}Au(α, *f*) and ^{197}Au(α, *xnyp*) reactions and from room background.

The averaged α-beam current during the stack irradiation was determined in two independent ways (see Sect. 2): (*i*) from the comparison of the activities of the two thin Al foils and (*ii*) from the measured ^{22,24}Na activities in the inserted Al monitor foils, using experimental ^{27}Al (α, *xnyp*) cross sections [6]. The results of the methods (*i*) and (*ii*) agreed within 6%; their mean value has been adopted. The decrease of the α-particle beam intensity within the stack due to nuclear reactions was calculated from geometrical cross sections; the accumulated effect reaches 2.5% at the last foil. The α-particle energy for the middle of each Au or Al foil was derived from the primary cyclotron-beam energy and the stack properties using the range tables given in Ref. [7].

The escape of fission fragments from the Au foils was estimated as follows: Assuming isotropic angular distribution, elementary geometrical considerations yield a mean escape probability of 1/4 for a fragment produced in a surface layer with a thickness equal to the range of the fragment. For each type of fission product the mean kinetic energy per mass unit was calculated using text-book fundamentals [8, 9]. Mean ranges were then obtained from the tables of Ref. [10] applying a small correction for Z_{medium} oscillations [11] of the stopping power. Escape fractions of 0.11–0.14 (two-sided) were finally derived for the

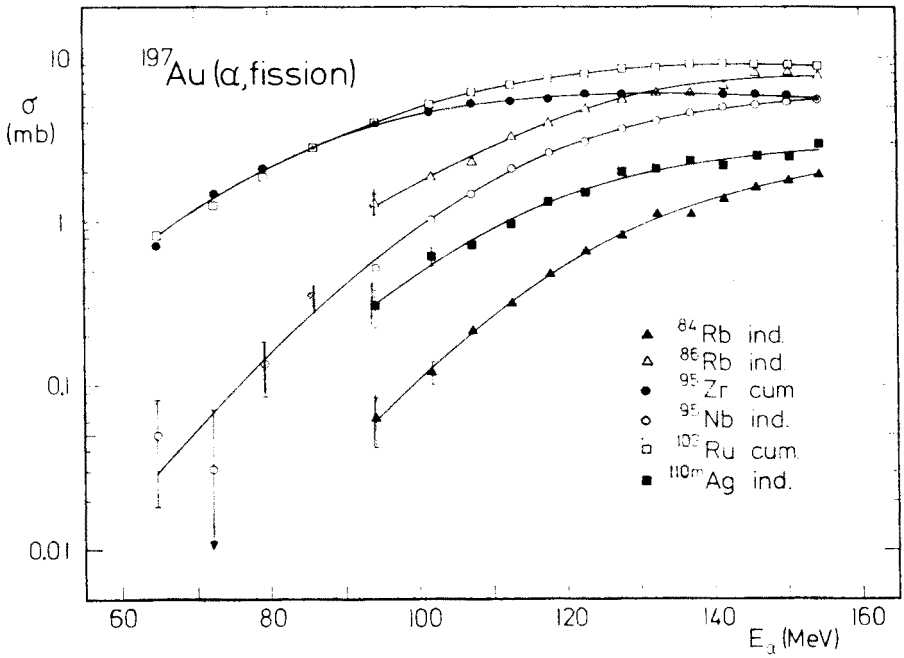

Fig. 1. Experimental yields for the production of some fission products in higher-energy α-particle induced fission of gold

TABLE II

Experimental yields of fission products from ^{197}Au (α, *fission*); information on errors can be found in the text and in Fig. 1

E_α (MeV)	σ (mb)					
	^{84}Rb	^{86}Rb	^{95}Zr (cum.)	^{95}Nb	^{103}Ru (cum.)	^{110m}Ag
64.7			0.716	0.050	0.809	
72.3			1.50	0.031	1.36	
79.3			2.11	0.135	2.07	
85.9			2.79	0.358	2.83	
94.1	0.063	1.30	4.00	0.527	4.05	0.304
101.7	0.121	1.88	4.66	1.03	5.17	0.623
107.2	0.219	2.30	5.28	1.49	6.18	0.718
112.6	0.323	3.30	5.47	2.11	6.82	0.967
117.8	0.478	3.98	5.60	2.64	7.41	1.32
122.8	0.664	4.87	6.08	3.09	7.92	1.49
127.7	0.825	5.63	6.01	3.71	8.57	1.99
132.4	1.13	6.11	6.00	4.09	8.75	2.09
137.0	1.12	6.07	6.04	4.54	9.08	2.34
141.5	1.36	6.73	5.97	5.00	9.16	2.18
145.9	1.62	8.12	6.06	5.11	9.16	2.52
150.2	1.78	8.23	5.74	5.33	8.95	2.44
154.4	1.91	7.78	5.47	5.47	8.85	2.97

present experimental conditions. These numbers are rather independent from the α-particle energy and from assumptions about the fission process; their uncertainty ($\simeq 3\%$) is mainly due to the errors attributed to the range tables [10]. The calculated escape fractions were confirmed experimentally by comparing the γ-ray spectra of adjacent Au and Cu foils (see Sect. 2).

The experimental results are shown in Fig. 1; numerical values are given in Table II. Four independent and two cumulative excitation functions of the ^{197}Au (α, f) process are given over a 60–90 MeV wide E_α-range. The errors in the cross sections are composed of the statistical errors in the areas of peaks in the γ-ray spectra and an additional error of 7% for all points which contains contributions from the α-beam intensity, the Ge(Li)-spectrometer efficiency and the target thickness; contributions from the spectroscopic data of Table I can be neglected. The errors in the α-particle energies originate from the foil thicknesses and the range tables used. The uncertainty of the foil thicknesses of about 1.5% induces errors of up to 2 MeV in the E_α-values. The range tables [7] are stated to be correct within 5%. According to previous experience [1, 12], this is certainly too pessimistic for our case; we adopt an uncertainty of 2% in the tables which, together with the other effects, gives rise to errors of up to 3 MeV for the lower α-particle energies.

4. Analysis of the data for the mass chain A = 95

If one considers the ratio between the independent yield of $^{95}_{41}$Nb and the cumulative yield of $^{95}_{41}$Zr (see Fig. 1), it turns out to increase from 0.04 to 1.0 in the present α-energy range. This qualitatively indicates a narrow charge distribution and/or a strong energy dependence of the most probable charge. Unfortunately it is not possible to derive the width of the charge distribution from only two measured yields within one mass chain with sufficient accuracy. Because of the scarcity of data in this energy region, it nevertheless seemed worthwhile to perform an analysis in a somewhat restricted scope.

The analysis was applied to smoothed data sets taking the yield values at $E_\alpha = 65, 75, 85, \ldots, 155$ MeV from the curves in Fig. 1. As a first step, the measured yields for Zr and Nb were assumed to represent together the total chain yield; in other words: the formation of ^{95}Mo, which is stable and not measurable with the present method, was neglected. For each E_α-value, fractional yields could now be calculated which then were used to determine the most probable charge. For this purpose the usual assumption was made that the charge distribution is a Gaussian [13, 14]:

$$P(Z) = (c\pi)^{-1/2} \exp\left(-(Z-Z_p)^2/c\right).$$

Here, $P(Z)$ is the fractional independent yield, c is the width constant of the charge distribution and Z_p is the most probable charge. For the fractional cumulative yield the corresponding integral [13, 14] over this expression was taken. The solid lines in Fig. 2 show these relations; the usual plot of "the logarithm of the fractional yield" against "$Z-Z_p$" permits a simple simultaneous presentation of data at different energies. The value $c = 0.95$ has been adopted from McHugh and Michel [15] who investigated ^{232}Th $(\alpha, \textit{fission})$ at $E_\alpha \leqslant 40$ MeV. Amongst the systems for which charge-distribution widths have been

determined this one is nearest to the present situation[1]. The $Z_p(E_\alpha)$-values as derived from the fractional independent yield of ^{95}Nb and from the fractional cumulative yield of ^{95}Zr turned out to agree at $E_\alpha = 65$ MeV and to differ by 0.12 charge units at $E_\alpha = 155$ MeV. This deviation is assumed to be due to the neglect of the ^{95}Mo formation (see above). The mean Z_p-values (from the ^{95}Zr and the ^{95}Nb data) were used to calculate the ^{95}Mo yield. This turned out to be negligible at $E_\alpha = 65$ MeV and to amount to 6.5% of the total chain yield at $E_\alpha = 155$ MeV.

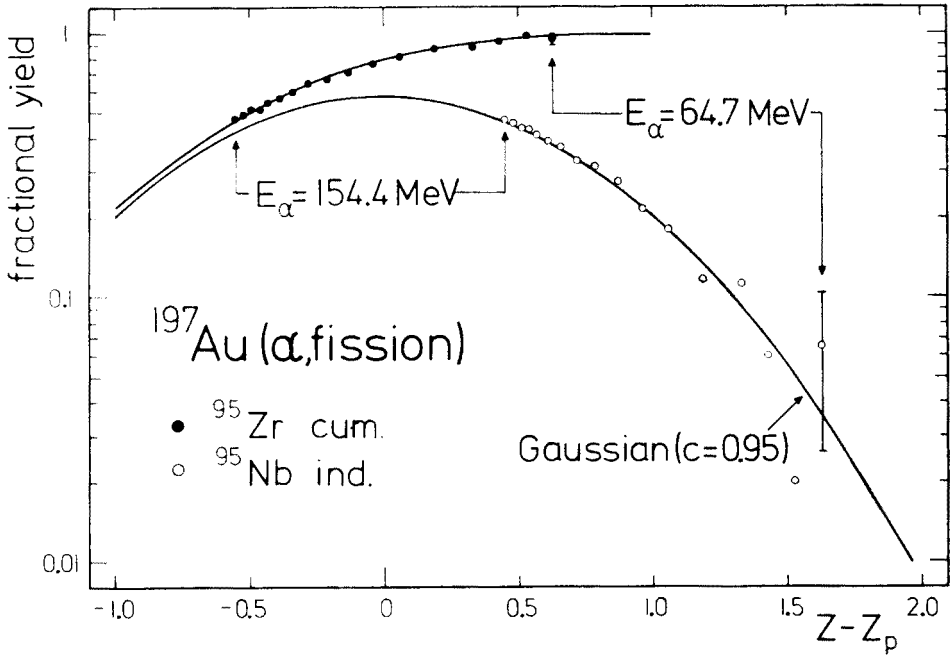

Fig. 2. Fractional independent yield (lower curve) and fractional cumulated yield (upper curve) for a Gaussian charge distribution as functions of Z–Z_p; for details on the experimental points see text

As a second step, the determination of the $Z_p(E_\alpha)$-values was repeated, starting this time from the experimental fractional yields corrected for ^{95}Mo formation. Now, at each energy in the whole range, the Z_p values from the ^{95}Zr and those from the ^{95}Nb data agreed very well (within 0.01 charge units) with each other and also with the averaged results of the first step. Fig. 3 shows the energy dependence of Z_p (solid line); as mentioned above, smoothed data sets were used in the evaluation. The points in Figs. 2 and 3 indicated as experimental data have the following meaning: In Fig. 2 the points represent the experimental fractional yields corrected for ^{95}Mo formation; their Z_p-values were taken from the smoothed-data curve in Fig. 3 in order to avoid non-monotonic $Z_p(E_\alpha)$-dependences

[1] In order to extract c-values for the present case the experimental set-up has been modified to measure three isobaric yields for the $A = 95$ and 105 mass chains. Preliminary results are given in Ref. [16]; a detailed paper will be published.

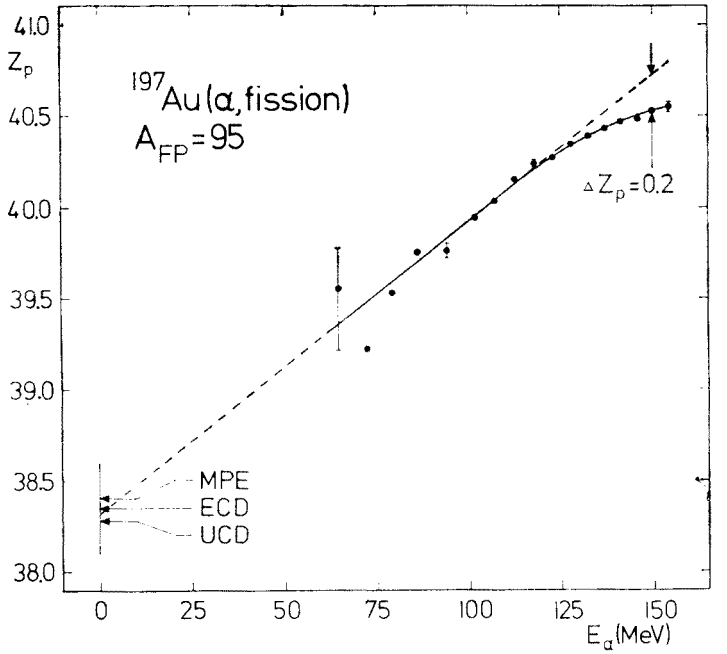

Fig. 3. Energy dependence of the most probable charge within the mass chain $A = 95$ in ^{197}Au (α, *fission*); the solid line was derived from smoothed experimental yields (see Sect. 4). The labels MPE, ECD, UCD and ΔZ_p are explained in the text

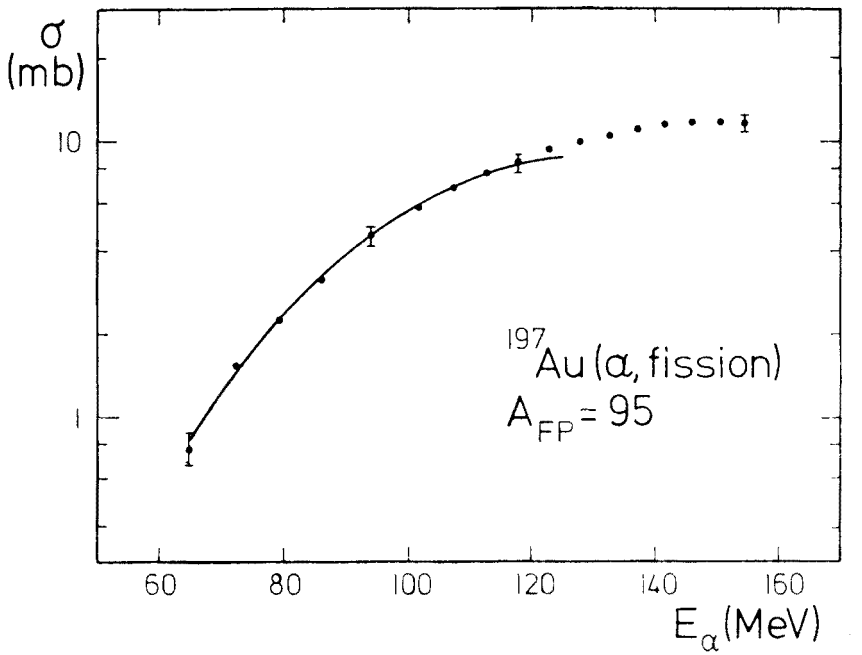

Fig. 4. Comparison of the total yield for the mass chain $A = 95$ based on the present data (points) with that derived from experiments [2] using fission-fragment detectors (solid line)

for the sake of clearness. The points in Fig. 3 represent Z_p-values derived from the corrected experimental fractional yields. The errors shown do not include contributions from an uncertainty of the c-value. For $\Delta c = \pm 0.05$ [15] these would be negligible in the present energy range.

It is interesting to compare also the absolute yields for the mass chain $A = 95$ with the results of other investigations. Such a comparison is shown in Fig. 4. The points give the present results (including the correction for ^{95}Mo formation). The solid line was derived from data based on fission-fragment detector experiments and reported by Moretto [2]. In this derivation a Gaussian mass distribution with a width of 20 mass units [17] was assumed for the whole energy range. The shift of the distribution as a function of α-particle energy was taken into account using the measured Z_p-dependence; this correction, however, is almost negligible because the chain yields are rather A-independent in the neighbourhood of symmetric fission.

5. *Discussion and summary*

The linear part of the curve (solid line) in Fig. 3 can be interpreted as result of the shift of the fission-product distribution due to neutron evaporation. Its slope corresponds [15] to an amount of energy of $\Delta E_\alpha = 12.5$ MeV per emitted neutron. The present experiment can of course not differentiate between pre- and post-fission emission. The linear part of the curve has been extrapolated both to lower and to higher energies (dashed lines). The labels MPE, ECD and UCD denote the Z_p-predictions of three simple models for low-energy fission: Minimum Potential Energy, Equidistant Charge Displacement and Universal or Unchanged Charge Distribution [14, 15]. In the present case of nearly symmetric fission these models yield almost identical predictions. This comparison should only demonstrate a kind of overall consistency; information on the Z_p-behaviour at lower energies can of course not be derived from the present data.

At the highest energies under consideration the E_α-dependence of Z_p deviates distinctly from the above linearity: The most probable charge increases more slowly with energy. This feature could be explained taking into account an increasing probability for precompound emission of nucleons. There are two ways how such an effect could become relevant: Firstly, precompound emission requires more energy which reduces the number of emitted neutrons per energy unit. Secondly, precompound proton emission counteracts the dominating neutron emission in decreasing the most probable charge. In connection with the investigation of ^{197}Au (α, *xnyp*) excitation functions [1] a hybrid-model calculation has been performed [18] which showed how the reaction ^{197}Au + α proceeds via the different intermediate nuclei. At $E_\alpha = 150$ MeV this calculation predicts a precompound effect (combining both aspects mentioned above) which is of the same magnitude as the observed deviation ($\Delta Z_p = 0.2$ in Fig. 3). For a more stringent comparison one would need calculations with a detailed treatment of nucleon emission and fission along the reaction chain; see, e.g., Ref. [19].

The energy dependence of the most probable charge Z_p within a given mass chain reflects the shift of the "island of fission products" within the nuclidic chart due to increasing

energy. Turning things around, it is in principle possible to derive from Fig. 3 information on changes in the location of the fission-product distribution with energy. In the case of data for only one mass chain, however, additional assumptions have to be made, such as: The "large axis" of the fission-product distribution is parallel to the stability line (ECD) for all energies; or: At a given projectile energy the Z_p-shifts are identical for all fission-product mass numbers. In these circumstances one obviously cannot yet draw sound conclusions on the fission-product distribution as a whole.

The results of the preceding sections may be summarized as follows: The yields for the formation of six fission products in higher-energy α-particle induced fission of gold have been measured over a 60–90 MeV wide energy range. The data for the mass chain $A = 95$ have been analysed with respect to the charge distribution and especially to the most probable charge and its energy dependence. In the analysis the charge-distribution width measured for a somewhat similar system was used ($c = 0.95$). The energy dependence of the most probably charge can qualitatively be understood as a result of nucleon (mainly neutron) emission with an indication of precompound effects at higher incident energies. Assuming a plausible value for the width of the mass distribution the absolute chain yield ($A = 95$) agrees with the result of an experiment using a quite different technique.

The authors would like to thank Mr. H. M. Jäger for his technical assistance.

REFERENCES

[1] A. Djaloeis, P. Jahn, H. J. Probst, C. Mayer-Böricke, *Nucl. Phys.* **A250**, 149 (1975).
[2] L. G. Moretto, *Physics and Chemistry of Fission 1973*, IAEA, Vienna 1974, Vol. I, p. 329.
[3] J. T. Routti, S. G. Prussin, *Nucl. Instrum. Methods* **72**, 125 (1969).
[4] L. L. Riedinger, N. R. Johnson, J. H. Hamilton, *Phys. Rev.* **C2**, 2358 (1970).
[5] W. W. Bowman, K. W. MacMurdo, *Atom. Nucl. Data Tables* **13**, 89 (1974).
[6] U. Martens, G. W. Schweimer, Report KFK 1083, Kernforschungszentrum Karlsruhe (1969); *Z. Physik* **233**, 170 (1970).
[7] C. F. Williamson, J.-P. Boujot, J. Picard, Rapport CEA-R3042, CEN Saclay 1966.
[8] M. Lefort, *Nuclear Chemistry*, Van Nostrand, London 1968, Chs. 6 and 7.
[9] R. Vandenbosch, J. R. Huizenga, *Nuclear Fission*, Academic Press, New York — London 1973, Ch. X.
[10] L. C. Northcliffe, R. F. Schilling, *Nucl. Data Tables* **A7**, 233 (1970).
[11] D. Ward, J. S. Forster, H. R. Andrews, I. V. Mitchell, G. C. Ball, W. G. Davies, G. J. Costa, Report AECL-5313, Chalk River 1976.
[12] H. J. Probst, S. M. Qaim, R. Weinreich, *Int. J. Appl. Radiat. Isotopes* **27**, 431 (1976).
[13] A. C. Wahl, R. L. Ferguson, D. R. Nethaway, D. R. Troutner, K. Wolfsberg, *Phys. Rev.* **126**, 1112 (1962).
[14] Ref. [9], Ch. XI.
[15] J. A. McHugh, M. C. Michel, *Phys. Rev.* **172**, 1160 (1968).
[16] P. Jahn, S. M. Sahakundu, H. J. Probst, C. Alderliesten, C. Mayer-Böricke, Int. Symp. on Physics and Chemistry of Fission, Jülich, FRG, 14–18 May 1979, "Extended Synopses", IAEA-SM/241-C23, p. 105.
[17] F. L. Lisman, H. W. Brandhorst, Jr., J. W. Cobble, *Phys. Rev.* **140**, B863 (1965).
[18] P. Jahn, Institut für Kernphysik, Kernforschungsanlage Jülich, Annual Report 1975, KFA-IKP 10/76, p. 39.
[19] J. J. Hogan, E. Gadioli, E. Gadioli-Erba, C. Chung, *Phys. Rev.* **C20**, 1831 (1979).